ACCOUNTS
of chemical research

# Kinetic and Energetic Paradigms for Dye-Sensitized Solar Cells: Moving from the Ideal to the Real

BRIAN C. O'REGAN* AND JAMES R. DURRANT
*Department of Chemistry, Imperial College London, Exhibition Road, London SW7 2AZ, United Kingdom*

RECEIVED ON MAY 5, 2009

## CONSPECTUS

Dye-sensitized solar cells (DSSCs) are photoelectrochemical solar cells. Their function is based on photoinduced charge separation at a dye-sensitized interface between a nanocrystalline, mesoporous metal oxide electrode and a redox electrolyte. They have been the subject of substantial academic and commercial research over the last 20 years, motivated by their potential as a low-cost solar energy conversion technology. Substantial progress has been made in enhancing the efficiency, stability, and processability of this technology and, in particular, the interplay between these technology drivers. However, despite intense research efforts, our ability to identify predictive materials and structure/device function relationships and, thus, achieve the rational optimization of materials and device design, remains relatively limited.

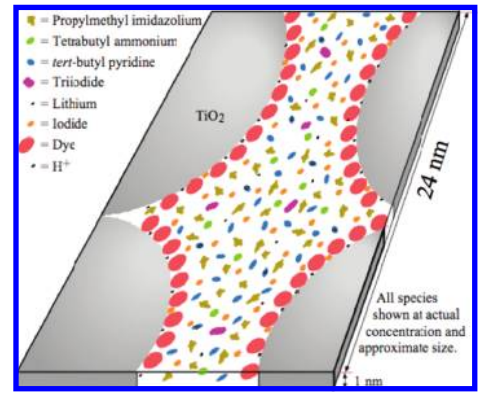


A key challenge in developing such predictive design tools is the chemical complexity of the device. DSSCs comprise distinct materials components, including metal oxide nanoparticles, a molecular sensitizer dye, and a redox electrolyte, all of which exhibit complex interactions with each other. In particular, the electrolyte alone is chemically complex, including not only a redox couple (almost always iodide/iodine) but also a range of additional additives found empirically to enhance device performance. These molecular solutes make up typically 20% of the electrolyte by volume. As with most molecular systems, they exhibit complex interactions with both themselves and the other device components (e.g., the sensitizer dye and the metal oxide). Moreover, these interactions can be modulated by solar irradiation and device operation. As such, understanding the function of these photoelectrochemical solar cells requires careful consideration of the chemical complexity and its impact upon device operation.

In this Account, we focus on the process by which electrons injected into the nanocrystalline electrode are collected by the external electrical circuit in real devices under operating conditions. We first of all summarize device function, including the energetics and kinetics of the key processes, using an "idealized" description, which does not fully account for much of the chemical complexity of the system. We then go on to consider recent advances in our understanding of the impact of these complexities upon the efficiency of electron collection. These include "catalysis" of interfacial recombination losses by surface adsorption processes and the influence of device operating conditions upon the recombination rate constant and conduction band energy, both attributed to changes in the chemical composition of the interface. We go on to discuss appropriate methodologies for quantifying the efficiency of electron collection in devices under operation. Finally, we show that, by taking into account these advances in our understanding of the DSSC function, we are able to recreate the current/voltage curves of both efficient and degraded devices without any fitting parameters and, thus, gain significant insight into the determinants of DSSC performance.

## 1. Introduction

Dye-sensitized solar cells (DSSCs) are one of the solar technologies that promise lower costs for photovoltaic electricity. Inherent in the mechanisms by which DSSCs work is a tolerance of lower purity materials and lower cost processing steps. A fundamental study of DSSC function is interesting on two counts: (1) laying the founda-

Published on the Web 09/14/2009 www.pubs.acs.org/acr
10.1021/ar900145z CCC: $71.50 

tions for enhanced device performance and (2) advancing surface science and electrochemistry in nanoporous electrodes. Considerable effort has gone into optimizing DSSC fabrication and finding new materials to improve efficiency. This has been paralleled by attempts to understand DSSC operation to better guide future development. Many of the basic characteristics have been described, and a conceptual model has grown up, which we will refer to as the "ideal model".[1,2] This model has had reasonable success in describing the various reactions and interactions in DSSCs but has had only limited success in contributing to the optimization of device performance. There is now an accumulation of data indicating some of the features of this "ideal model" may miss the real complexity of high efficiency DSSCs. In addition, the ideal model cannot describe some key features of the cell performance. In this Account, we focus on advances in our understanding of DSSC function and implications for materials and device optimization. Broad reviews of DSSCs have been published elsewhere.[1,3]

To come to grips with the chemical complexity in DSSCs, we have adopted an approach in which we measure the kinetic parameters of real operating cells, under illumination. Conclusions about the kinetics or other characteristics can then be checked against the actual cell performance. We also perform complete characterization of many cells with varying chemistry and fabrication. This allows us to detect features that have been missed by looking over a narrower range of chemistries and techniques. To accomplish this, we are automating and extending the typical tools used to study DSSCs, for example, spectral response, transient electrical characterization, and transient absorption spectroscopy.

In this Account, we consider four additions that we believe need to be made to the existing conceptual models. These are as follows: (1) Species adsorbed to $TiO_2$, specifically dye molecules and co-adsorbates, have the potential to "catalyze" the recombination reaction between electrons in $TiO_2$ and the electrolyte, reducing the open-circuit potential ($V_{oc}$) and even the photocurrent ($J_{sc}$). Previously, adsorbates have been discussed only in terms of their ability to block recombination. (2) The electron diffusion length in DSSCs is less than half as long as indicated by the current method of calculation. This has large implications for the estimation of recombination losses and for finding the optimum film thickness for different dyes, electrolytes, and cell structures. (3) Electron/electrolyte recombination, even for the same electron density, is accelerated by illumination. Although perhaps not surprising, this effect is not included in the standard conceptual model. Quantification of the degree of acceleration has allowed us to simulate the

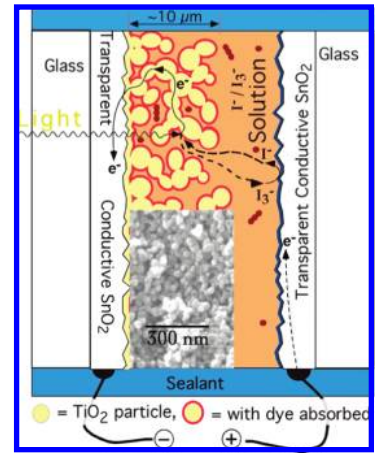


**FIGURE 1.** Physical schematic of a DSSC. (Inset) SEM of the $TiO_2$.

shape of the JV and understand the determinants of the fill factor (FF). (4) The $TiO_2$ conduction band edge potential in a given cell shifts negative with increased illumination and/or applied bias. This effect, difficult to explain with the standard assumptions about the electrolyte in the pores, nonetheless seems the best way to explain some obvious features of DSSCs. If true, this would allow current models of electron trapping in $TiO_2$ to correctly simulate recombination in DSSCs.

Because of space limitations, we focus only on issues relating to electron recombination and collection. We have discussed issues relating to electron injection and regeneration elsewhere.[4,5]

## 2. Overview of DSSC Function

**2.1. Cell Construction.** A typical research DSSC is shown in Figure 1, as reviewed elsewhere.[6] From left to right, the cell consists of a transparent conductive oxide (TCO) substrate, normally doped $SnO_2$ on glass. A porous transparent semiconductor layer is coated onto the substrate, normally 10−15 $\mu$m of ~20 nm $TiO_2$ particles, which gives an internal surface area of ~1000 $cm^2$ per $cm^2$ substrate. Dye molecules are absorbed onto the internal surface of this semiconductor to make approximately one monolayer. The standard dye is N719 (Figure 3). The substrate is joined to a counter electrode, normally a few nanometers of platinum on another TCO glass. A seal is formed around the cell, followed by injection of electrolyte through a hole and sealing of the hole. All record cells thus far have been based on an iodine/iodide electrolyte in organic solvent. A typical electrolyte consists of methoxypropionitrile (MPN) with 0.6 M propylmethylimidazolium iodide, 0.1 M LiI, 0.1 M *tert*-butylpyridine, and 0.1 M iodine.

Many variants of the fabrication are possible, including surface layers on $TiO_2$ particles (e.g., $Al_2O_3$), co-adsorbates put on with the dyes, and gelation agents in the electrolyte. Other

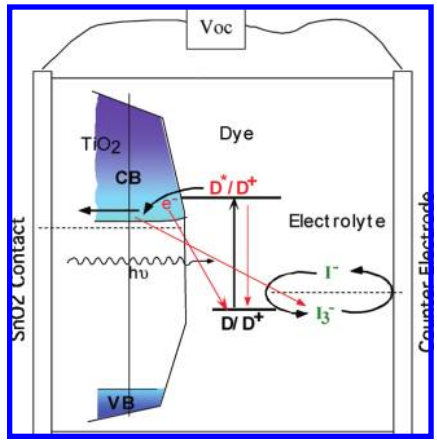


**FIGURE 2.** Forward and reverse electron-transfer steps in a DSSC.

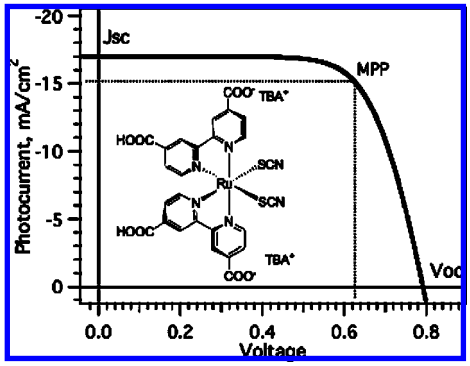


**FIGURE 3.** Idealized current versus voltage (JV) output from an efficient DSSC. (Inset) Structure of the standard dye, N719.

variants of the cell include depositing the $TiO_2$ layer on metal or using metal and/or carbon layers for the counter electrode. None of these change the basic functions of the cell described below.

**2.2. Cell Function.** We describe here a simplified picture of cell function. Figure 2 shows a schematic of the electron-transfer steps. We will discuss the additional complexities of real cells in section 3. Because DSSCs are designed to produce power, in this Account, we have chosen to focus on the function of DSSCs under the operating condition. This condition is the maximum power point (MPP), the point along the current versus voltage relationship (Figure 3) where the maximum power is extracted from the cell. Power production in a DSSC starts with the absorption of photons by the dyes. The transfer of an electron from the dye excited state to $TiO_2$ is termed electron injection. Injection is in competition with the decay of the excited state by luminescence, thermal decay to ground, or quenching. Injection leaves the dye in an oxidized state, which in turn oxidizes iodide from the electrolyte, a step referred to as regeneration. Regeneration is in competition with reduction of the oxidized dye by an electron from $TiO_2$. Under illumination, electron injection causes an increase in

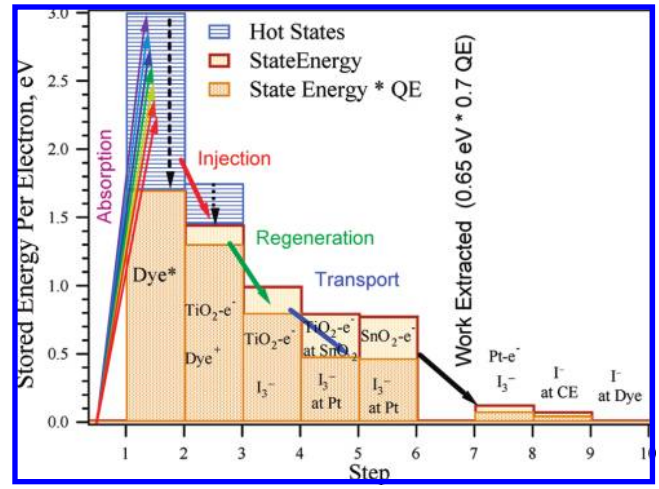


**FIGURE 4.** State energy diagram of a typical DSSC under 1 sun illumination at the MPP. Energy and quantum efficiency values are approximate and will change depending upon dye and electrolyte composition.

electron density in the $TiO_2$. If the cell is short-circuited or at the MPP, the $SnO_2$ provides a sink and a gradient in electron density will build up causing diffusive transport to the $SnO_2$. During transport, electrons can also be transferred back to the oxidized species in the electrolyte, termed recombination with the electrolyte. The photocurrent measured externally is the flux of injection minus the flux of both recombination reactions.

Figure 4 illustrates the energy costs of each step of device function. The higher level bars are the state energies given the electron and hole positions after each step. The solid bars are this same energy, reduced by the quantum efficiency losses up to that point, specifically for the MPP situation. The differences between the successive solid bar shows how much each step costs in a real cell under operation. Thus, large steps down on this graph indicate where research breakthroughs might cause large increases in cell efficiency. For the case illustrated, the MPP is assumed to correspond to a device voltage of 0.65 V and a photon to electron quantum efficiency of 0.7, yielding $0.65 \times 0.7 = 0.46$ eV of work extracted per absorbed photon. For a typical DSSC with the N719 dye, this yields a device efficiency of ~9.5% under AM 1.5 irradiation.

**2.3. Materials Characteristics.** It is useful, when discussing DSSCs, to have a general feel for the materials and the relative concentrations of various species in the particles and the adjacent pores. The following description is idealized in that it ignores known complexities to be described later. Figure 5 shows a schematic of the chemical species in a 1 nm thick slab through one pore, based on a typical electrolyte (solvent is omitted). The total volume fraction of the solutes in a typical electrolyte is ~20%. Interactions have not been taken into

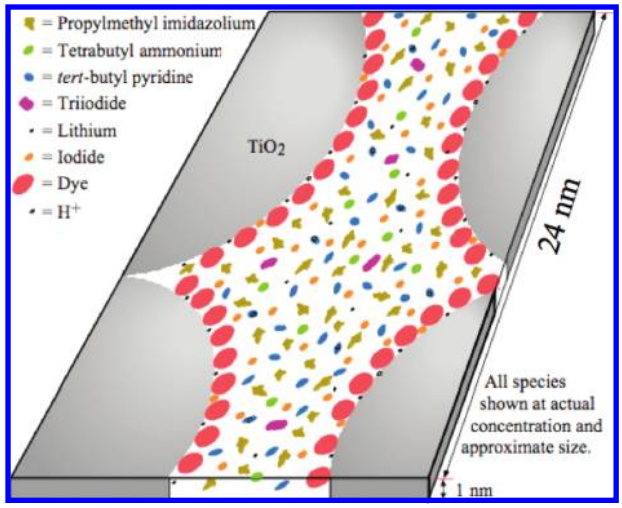


**FIGURE 5.** Diagram of a 1 nm slab sliced from a pore in a typical DSSC (the tetrabutylammonium originates from the N719 dye).

account, except the known binding of $H^+$ and $Li^+$ to $TiO_2$ and that iodine binds very strongly to iodide forming $I_3^-$. The concentration of "unbound" iodine is <1 $\mu$M. A $TiO_2$ particle, diameter of 18 nm, has ~600 dyes on the surface. At 1 sun illumination, each dye (assuming N719) absorbs a photon only once per second. Thus, the flux of electron injection into the particle is ~600 $s^{-1}$. Regeneration times are ≤10 $\mu$s, meaning ≤1/100 000 dyes is in the oxidized state or ≤1 per 150 particles. In the pore volume around a particle, there will be ~1000 iodide atoms and 200 $I_3^-$ molecules. If the pore composition is similar to the bulk, there will be about 1 free iodine per 10 000 particles. The $TiO_2$ layer contains defects that act as electron traps. According to electrochemical measurements, the trap density forms an exponential tail below the conduction band containing ~30 traps per nanoparticle over the energy range covered by DSSCs.[7] Thus, there are two populations of electrons in the cell, those in the traps (>90%) and those in the conduction band (<10%). Also, because of the small size of the nanoparticles and high conductivity of the electrolyte, it is not possible to have a significant electric field across individual particles or across the entire $TiO_2$ film. Thus, in normal DSSCs, charges in both phases move by diffusion rather than drift.

In the following, we will refer to the "applied potential" of the cell, the Fermi level in the $TiO_2$, and the concentration of electrons in the $TiO_2$. All of these terms are related. The electrochemical potential of the electrolyte is well-buffered by the high concentration of oxidized and reduced forms and does not change significantly under operation. The redox potential of the electrolyte forms the zero of any measure of potential in the cell. Applying a negative potential to the $TiO_2$ (equivalent to adding a load and extracting power) raises the Fermi level in the $TiO_2$ toward the conduction band and increases the concentration of electrons in the traps and conduction band.

**2.4. Chemical Interactions.** A very important chemical interaction in DSSCs is the binding of electrolyte species to the $TiO_2$ surface. While rarely studied in itself,[8] this interaction has been empirically manipulated for over 15 years to increase the voltage output of the cell. $TiO_2$ is reactive and binds most of the species in the electrolyte to some degree. Taken together, the ions bound to the surface will impart a net charge to the surface. This charge will be balanced by oppositely charged ions in solution, causing an electric field between the $TiO_2$ surface and the bulk of the electrolyte (see Figure 6). As an example of the magnitude of this effect, $TiO_2$ has been found to have ~10 binding sites for $H^+/nm^2$, implying ~10 000 sites for $H^+$ absorption on an 18 nm particle. More bulky adsorbates will have lower saturation density. This can be compared to the number of electrons in the particle under operation, which is never more than 30. It is clear that understanding the absorption/desorption of ions is critical to understanding cell function. The standard theory of non-interacting charges predicts that the concentrated electrolyte will confine the effect of the surface charge to within a few nanometers of the metal oxide surface. The center of the pores would thus have the same characteristics as the bulk electrolyte. Recent results call this assumption into question.[9] Given that the volume fraction of solutes in the typical electrolytes is ≥20% and that the pore necks are as little as 10 solvent molecules across, surface effects on the full pore volume probably can occur.

Another important interaction, only recently appreciated, is that iodine binds to the dye molecules. This binding can accelerate the recombination reaction, significantly reducing the $V_{oc}$ and $J_{sc}$.[10] Also, iodide has recently been suggested to form a complex with the oxidized dye, and another as yet unidentified species binds to the ground-state dye. Lastly, there will be a degree of ion pairing between all opposite charges in the electrolyte. It is important to note that all of these associations come into equilibrium in the dark, forming the "ground state" of the cell. Of particular interest are molecular associations that may change under operation, by either the action of light or applied voltage. For example, the current through the cell might involve dissociation of a given complex. If the reformation rate of this complex is slow enough, there could be a change in the average degree of association. If that then changes the equilibrium of ions absorbed on the $TiO_2$, the band offset may change with the application of illumination or potential. Possible examples of this effect are discussed below.

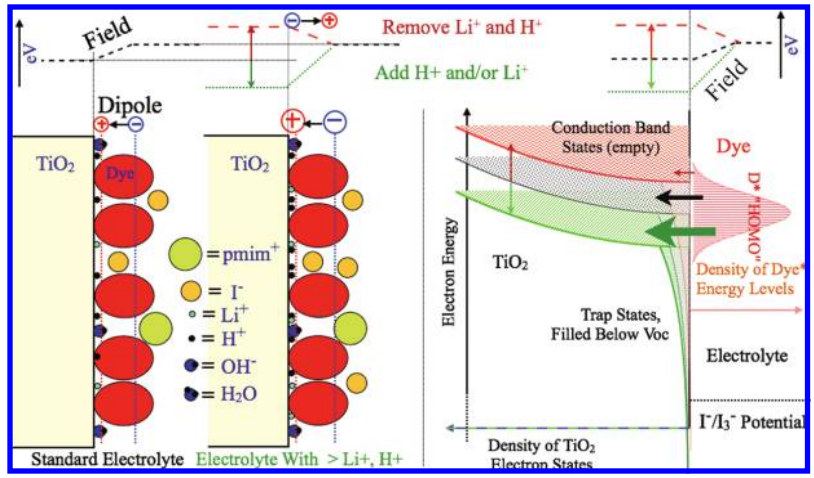


**FIGURE 6.** (Left) Schematic of the $TiO_2$/electrolyte interface showing changes in surface binding and resulting electric field. (Right) Density of states versus energy diagram showing band edge shifts and changes in the injection rate that can result.

## 3. Electron Collection and Recombination: Recent Advances

In this section, we present the more complicated details of DSSCs, as they are emerging from new measurements from our own laboratory and others. Because of space limitations, we focus on how transport and recombination of electrons and the surface electric field combine to determine the $V_{oc}$ and the shape of the JV curve. We will use the terms recombination lifetime and recombination rate constant. By "rate constant", we always mean the pseudo-first-order rate constant, which is the inverse of the lifetime. Charge densities have been determined by charge extraction,[11,12] and the recombination lifetime is from small perturbation photovoltage decays.

**3.1. Open-Circuit Potential.** As in any solar cell, the open-circuit potential is defined by the point where the flux of recombining charges is equal to that of charge generation (electron injection in the case of DSSCs). In principle, because charge transport makes minimal contribution to the open-circuit potential, the open-circuit condition is simpler to characterize than the short circuit or MPP. In practice, there are large number of variables known to control the $V_{oc}$, and more are still being discovered.

The two main determinants of $V_{oc}$ are the recombination rate constant and the $TiO_2$ conduction band edge offset relative to the $I^-/I_3^-$ midpoint potential. Under illumination, the electron concentration in the $TiO_2$ increases until it creates a recombination flux equal to the injection flux. The free energy of the $TiO_2$ electrons is expressed by the position of the Fermi level in the semiconductor. The measured $V_{oc}$ is the difference between the free energy of the electrons at this "dynamic equilibrium" concentration and the electrolyte potential. The recombination flux is the recombination rate constant multiplied by the charge ($U_{rec} = k_{rec}n$). Clearly, if the recombination rate constant increases, then for a given injection flux, the concentration at equilibrium will decrease, along with the free energy of the electrons and, thus, the $V_{oc}$. The effect of the band offset is more subtle. In a $TiO_2$ material with no defects, all of the injected electrons reside in the conduction band and the Fermi level is located below the conduction band edge by an amount that only depends upon the electron concentration (for a given material). A given $n$ will give a particular $V_{oc}$. If we insert or change the electric field between the $TiO_2$ and the electrolyte, we simply move all of the states in the $TiO_2$ relative to the electrolyte, including the conduction band and Fermi level (Figure 6). For the same $n$, we will measure a difference in $V_{oc}$ identical to the change in the electric field at the $TiO_2$ surface. This assumes that everything else remains equal, including electron injection, regeneration, and recombination rate constant. In the trap-rich $TiO_2$ used in DSSCs, the situation is identical, except that the charge density for a given Fermi level is determined by the distribution of electron traps. The normal assumption is that changing the surface electric field does not change the energy distribution of the traps relative to the conduction band, and thus, we again expect a change in $V_{oc}$ to match any change in the conduction band offset.

The simple picture in the above paragraph hides a wealth of detail. Let us first discuss the recombination rate constant. It is possible that some fraction of the recombination could proceed via electrons trapped at defects on the surface (surface states). This has led to a discussion that electrolyte additives and dye molecules can act to block recombination from these sites, decreasing the overall rate and increasing the $V_{oc}$. Little note has been taken of the cases where the additives resulted in a lower voltage. The reduction of iodine or $I_3^-$ is a complex two-electron reaction. On bare $TiO_2$, the reduction

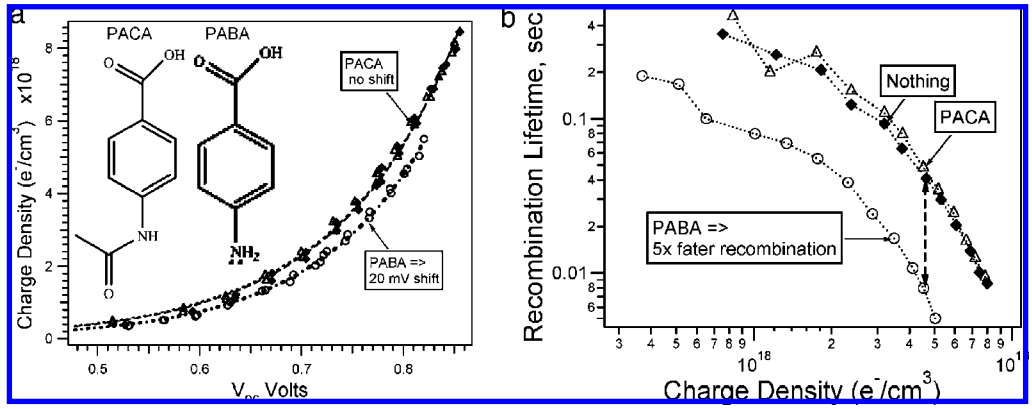


**FIGURE 7.** (a) Electron density in $TiO_2$ versus $V_{oc}$ for various electrolyte additives. (b) Recombination lifetime versus electron density for the same cells.

of $I_3^-$ and/or $I_2$ is very slow, thus even relatively weak stabilization of intermediates could have noticeable catalytic effects. We have recently found that both electrolyte additives and dyes can have an effect opposite of that intended, catalyzing the recombination. Some particularly bad dyes can cause 100-fold increases in the recombination rate constant, decreasing the $V_{oc}$ by hundreds of millivolts.[10] Initially, we noted that dyes that increase recombination have sites for binding iodine. Within otherwise equivalent dyes, the binding strength correlated with the increase in recombination.[12] More recently, we have found that even the standard dyes (e.g., N719) used in DSSCs bind iodine quite strongly without apparently catalyzing recombination. The mechanism for the acceleration of recombination must involve a combination of the strength of the iodine binding sites, their proximity to the $TiO_2$ surface, and probably catalysis of the reduction by stabilization of an intermediate.

To illustrate this effect, we examine the anomalous behavior of an electrolyte additive (PABA; Figure 7). PABA absorbs to $TiO_2$ via the carboxylate moiety. According to a study of similar benzoic acids (excluding PABA), the molecular dipole of PABA indicates that it should increase the $V_{oc}$ by shifting the band edge negative.[13] However, the actual effect on the $V_{oc}$ is a decrease of 40 mV. The effect of PABA on the band offset can be seen in Figure 7a. This figure shows the total electron density in the $TiO_2$ versus the $V_{oc}$, varying $V_{oc}$ by light intensity. This is equivalent to a map of the trap state density in the $TiO_2$ relative to the electrolyte redox potential.[11] Following the logic of Figure 6, a change in the surface electric field will cause an identical shift in the trap state distribution, which will show up as a shift in Figure 7a. This technique is often used to measure shifts in the surface field caused by dye molecules and additives.[14] The PABA cell does show a negative shift as expected from the dipole. Normally, this would increase the $V_{oc}$. To explain the drop in $V_{oc}$, we have to compare PABA to a similar molecule, PACA (Figure 7).

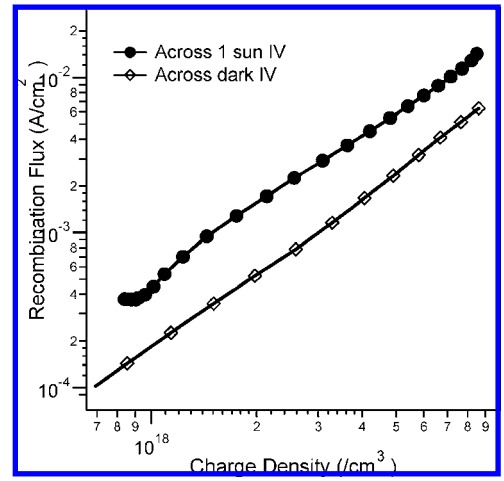


**FIGURE 8.** Electron/electrolyte recombination flux as a function of the electron density in the $TiO_2$, under dark, and 1 sun illumination.

The amine group on PABA should have an iodine binding constant of ~12.[15] On PACA, the binding has been reduced by the addition of an acetyl group. Acetamide has an iodine binding constant of only 0.6. This change also seems to decrease the molecular dipole because PACA does not cause a band offset (Figure 7a). In Figure 7b, the recombination lifetime versus charge is compared for cells with no additive, PABA, and PACA. The data show that PACA has no effect, whereas PABA decreases the recombination lifetime 5-fold, causing the observed drop in $V_{oc}$. In this case, the chemical effect, catalysis of recombination, overrides the physical effect of the molecular dipole.

To further complicate matters, we have found that the recombination rate for a given electron concentration in the $TiO_2$ is modified by the illumination intensity. To see this, we measure the charge density and recombination flux in a DSSC under applied voltages, in the dark and light. Typical data are shown in Figure 8. Open diamonds are the recombination flux in the dark (the dark current) versus charge density. Filled circles are the recombination current under illumination, at the same charge, estimated assuming all change in losses across

the JV is due to recombination (in other words, electron injection is independent of potential).[4] Uniformly across the JV, the recombination flux under 1 sun illumination is about twice that occurring in the dark, at the same electron density. We show below how this kind of data makes possible a more complete understanding of the JV shape.

With respect to the conduction band offset, things at first seem more in order. For example, the $V_{oc}$ has been shown to change with electrolyte composition in a fashion consistent with standard theories of adsorption and surface potential. However, there are still serious gray areas between theory and measurement. The darkest is the fact that the best theory of transport and recombination (known as the "multiple trapping model"[16]), which has been very successful in reproducing the transient behavior of the cell, fails to the give the correct relation between light intensity and voltage. The model predicts an "ideal" relationship of a 60 mV increase in $V_{oc}$ for each 10-fold increase in illumination. A few DSSCs are indeed "ideal" in this sense; however, most cells, including high-efficiency examples, are "non-ideal", showing 70−90 mV increases in $V_{oc}$ with each decade of light intensity. Tweaks to the model have been proposed to explain this effect, including arbitrary profiles of recombination from surface states and an "activity coefficient" for conduction band electrons.[17,18]

The prediction from the multiple trapping model is based on the assumption that the surface electric field does not change with illumination or current density. If one assumes an unchanging electrolyte composition, this assumption seems to be required by the high dielectric of $TiO_2$ and the electron concentrations involved. The issue has remained unresolved because there are as yet no direct measurements of the conduction band potential or *in situ* measurements of the surface charge under operation. Based on our recent measurements, however, it appears that the conduction band offset does change, in a given cell, as a function of operating conditions.

Our method to estimate the shifts in the conduction band is to measure the activation energy for recombination and/or transport as a function of the Fermi level in the $TiO_2$.[19] The assumption is made that the main contributor to the activation energy is detrapping in the $TiO_2$ to either the conduction band (or mobility edge) or some surface states at a fixed energy below the conduction band. Consistent with this, we have verified that the measured activation energy does increase appropriately (for a fixed Fermi level) when the band edge is shifted negatively by an intentional change in the adsorbed species.

To determine if the conduction band is moving in a given cell under operation, we have measured the activation energy ($E_a$) as a function of the cell $V_{oc}$. If the conduction band moves with applied bias or light level, the slope on the resulting plot (Figure 9) will deviate from −1.[19] We have found that the slope of $E_a$ versus $V_{oc}$ does indeed deviate from −1 and that the magnitude of this deviation correlates with the relation of $V_{oc}$ to light intensity in many cells (Figure 9). The simplest explanation is that the conduction band offset increases with either light or electron concentration. If correct, models of transport and recombination will need to incorporate this effect.

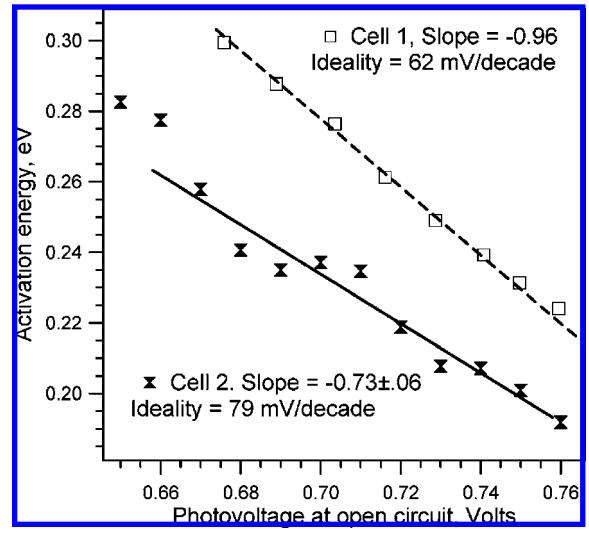


**FIGURE 9.** Measured activation energy versus open-circuit voltage. Lines are the trend predicted by the ideality (relationship of $V_{oc}$ to light intensity).

One explanation for this movement is that changes in the chemical equilibrium in the pores, dependent upon operating conditions, lead to shifts in surface charge. We have found that the ideality is controlled by at least the $TiO_2$ synthesis and the characteristics of the dye. The former could be consistent with an explanation of "non-ideality" based on an activity coefficient for the electrons, but the latter seems to support only an interface-based explanation.

**3.2. Short Circuit.** At short circuit, all of the available free energy in the charges is used to extract them with maximum quantum efficiency. This efficiency depends upon the diffusion constant (mobility) and recombination rate of the electrons in the $TiO_2$. Understanding the determinants of this efficiency is key to optimizing cell construction. For example, optimum $TiO_2$ film thickness depends in part on the relation of photocurrent losses to thickness.

Charge transport and recombination at short circuit occurs as follows. As electrons are injected from the dye, an electron density gradient builds up across the cell until it is large enough to carry all of the injected current to the "sink" at the $SnO_2$. Because transport in the $TiO_2$ is rather slow, the resulting electron density gradient results in a large average concentration of electrons in $TiO_2$ (on the order of $10^{18}$ $cm^{-3}$

$TiO_2$). This electron density causes a certain recombination flux. The size of this recombination flux relative to the injection flux gives the efficiency for photocurrent collection. A value often used to describe the relation of transport and recombination is the diffusion length. This is the length that an average charge will diffuse before recombining. If the diffusion length is less than the film thickness, the photocurrent efficiency will be low. Roughly, a diffusion length >2 times the film thickness implies most charges will reach the $SnO_2$ contact before recombining.

To estimate the photocurrent losses at short circuit, one can use the charge density and the charge lifetime. The former can be measured with charge extraction,[11] whereas the latter has been difficult to determine. A direct measurement of the recombination at $V = 0$ was proposed, referred to as "constant current transient photovoltage" (CCTPV).[7,20] From this measurement, it was found that the recombination rate was much slower at $V = 0$ than at $V_{oc}$. It was then suggested that the recombination rate was only dependent upon the electron density. If so, the recombination rate at short circuit, for a given light intensity, can be found by measuring the recombination rate at the open-circuit condition that has the same charge density. This is the current method for calculating diffusion lengths[21] and losses at $V = 0$.[7] The resulting diffusion lengths are much longer than the film thickness, giving the impression that recombination losses at short circuit are near zero for practically all DSSCs. However, based on the results in Figures 8 and 9, the method just described cannot be correct. If the light level has an effect on the recombination rate and the applied potential shifts the band edge, a lifetime from a different light level and bias cannot be used to calculate the diffusion length at short circuit.

A more robust way to find the diffusion length is to measure the difference in collection probability for electrons created far from and close to the collection electrode.[22,23] We have been extending this well-known concept to calculate accurate diffusion lengths for DSSCs.[24] The method involves measuring the photocurrent efficiency under different illumination wavelengths (spectral response) using light incident on the front or back of the cell (Figure 10). When the ratio of the spectral response from front and back illumination is combined with the measurement of the optical density at each wavelength, it allows for direct calculation of the diffusion length. Diffusion lengths measured in this way are ~2.5 times shorter than those measured by the method involving transport and recombination lifetimes. To test which diffusion length is correct, we have constructed cells with intentionally

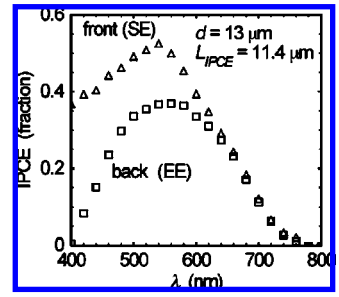


**FIGURE 10.** Example of the difference in spectral response between front (SE) and back (EE) illumination for a cell with the true diffusion length less than the film thickness (IPCE = incident photon to current efficiency). The previous method, see the text, gives a 30 $\mu$m diffusion length for this cell.[25]

varied recombination losses at short circuit. We find that the diffusion lengths calculated from the spectral response method correctly reproduce the measured photocurrent, whereas the diffusion lengths calculated by the previous method do not.[25] It appears now that optimized DSSCs with film thickness $\geq$16 $\mu$m are near the maximum thickness allowed by the current electrolyte compositions. This indicates that small changes in cell composition that reduce $J_{sc}$ may be causing this reduction by decreasing the diffusion length. Under the ideal conceptual model, the implied long diffusion lengths force any change in $J_{sc}$ to be ascribed to changes in light absorption or injection.

**3.3. MPP and the Shape of the JV.** Although the MPP is the operating point of the cell, it is much less studied than the short- or open-circuit condition. However, improvements in the fill factor of the cell are just as valuable as improvements in current or voltage. The study of changes in the MPP is also critical for understanding device aging by accelerated testing. We have begun a study of the shape of the JV by measuring the charge density as a function of voltage in the light and dark (Figure 11a). This unique data has allowed us to make a zero free parameter simulation of the complete JV of both normal and unusual cells.

To extract power from the cell, a load is placed on the circuit. This increases the voltage on the contacts relative to short circuit. This introduces a reverse (injection) current at the $SnO_2/TiO_2$ contact, reducing the net extraction efficiency. The effect is to increase the amount of charge in the $TiO_2$ for a given light level and current. We find that, in typical cells under 1 sun illumination at the MPP, the cell contains about twice the charge as at $V = 0$. There are roughly similar contributions from the charge built up by the diffusion gradient and that caused by the increased potential. Because the net extraction efficiency is not 1, losses in pho-

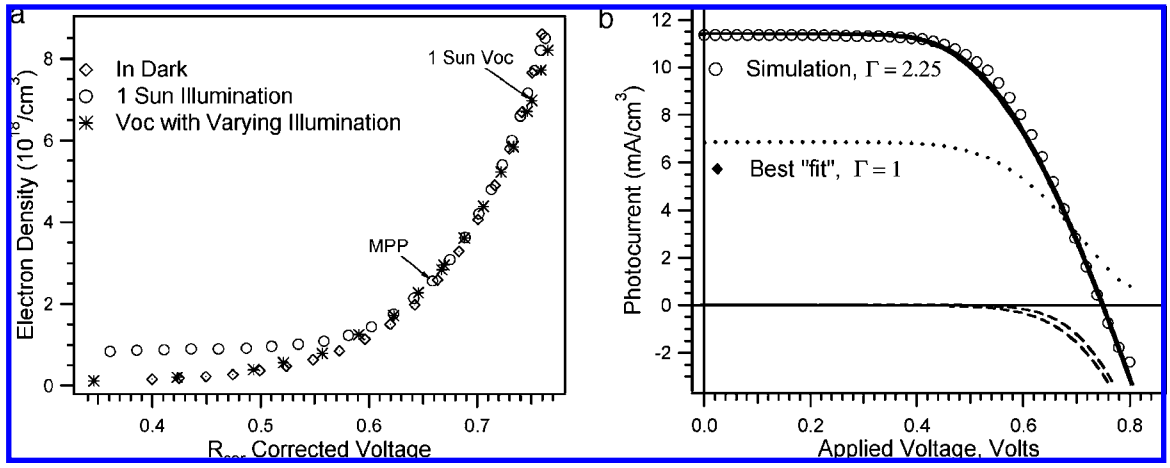


**FIGURE 11.** (a) Electron density in a typical DSSC as a function of applied potential. (b) Simulation of the JV of the same cell using eqs 1 and 2 and no fit parameters.

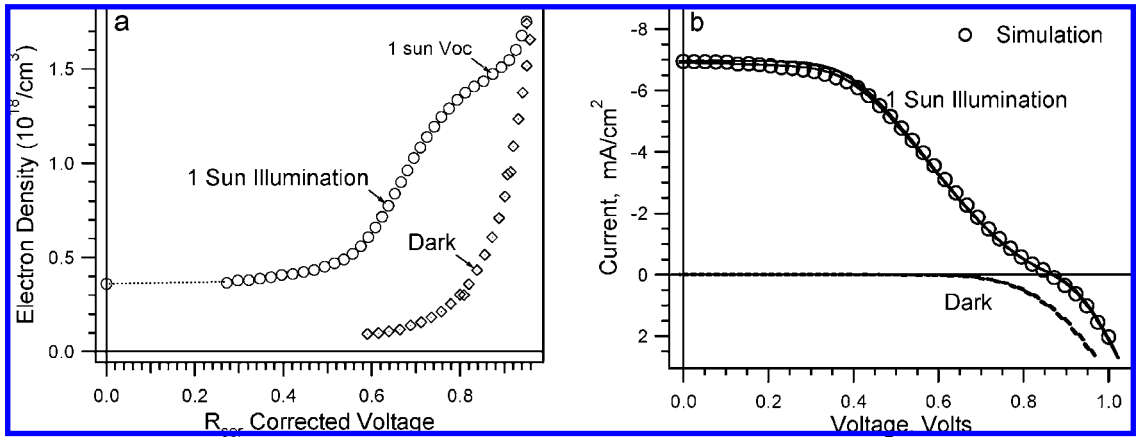


**FIGURE 12.** (a) Electron density in a degraded DSSC as a function of applied bias. (b) Simulation of the JV using eqs 1 and 2.

tocurrent at the MPP cannot be calculated from the diffusion length alone.

We combine some of the discoveries mentioned above to model the complete JV. We begin with the fact that the injection efficiency does not change significantly across the JV.[4] We then model the JV with

$$J(V) = J_{inj} - J_{rec}(V) \quad (1)$$

$$J_{rec}(V) = \Gamma\, k_{dark}(Q_{lt}(V))\, Q_{lt}(V) \quad (2)$$

For $J_{inj}$, we use $J_{sc}$ plus the collection losses at $V = 0$ indicated from the spectral response measurement above. $k_{dark}$ is the rate constant for recombination, as a function of charge, determined from the charge density measurements along the dark JV. $Q_{lt}(V)$ is the charge present at $V$, under illumination. $\Gamma$ is the difference factor between the recombination under dark and light, determined before the simulation from plots such as Figure 8. These equations and the measured charge data allow the entire JV to be simulated with zero fit parameters (Figures 11b and 12b).

Figure 11b shows the excellent simulation of a typical "good" cell. It is perhaps not surprising that we can simulate such a simple JV. However, the method also works on cells with materials that do not work perfectly, including degraded cells after stability testing. Figure 12b shows a cell over 1 year old that has developed an "S-shaped" JV. Figure 12a shows the charge versus voltage, light and dark. Unlike the cell in Figure 11, this cell shows an early onset of charge density, followed by a plateau. Nonetheless, eqs 1 and 2 model the JV perfectly. From this kind of result, one can narrow down the explanation for the degraded performance. For example, in Figure 12a, the charge along the dark IV increases in the normal fashion (Figure 11a). Thus, the anomalous increase in charge under light almost certainly occurs because the photoinjected electrons cannot escape from the $TiO_2$. This could come about due to a degraded $SnO_2/TiO_2$ contact or a degraded counter electrode. Explanations of the S-shaped IV involving increased density of trap states or an increased recombination rate constant can be ruled out.

## 4. Conclusions

The study of dye-sensitized cells seem poised to enter an era of much deeper understanding of the cell components and functions. We have discussed some of our recent results that may contribute to this watershed. We expect that the improved understanding will allow rational choice of new materials and structures, both raising the efficiency and improving manufacturability.

*This work was supported by the UK EPSRC (Grant EP/E035175/1) and the EU Seventh Framework Program (Grant 212792). We specifically acknowledge the contributions of Mindaugas Juozapavicius, Kate Walley, Virginie Vlissac, and Piers Barnes.*

### BIOGRAPHICAL INFORMATION

**Brian O'Regan** has been involved in renewable energy science since 1976 when he constructed and monitored a residential solar water heater. He began his studies on photoelectrochemistry of $TiO_2$ in 1987 at the University of Wisconsin, Madison, receiving a M.S. degree in 1990. After a year in the laboratory of Prof. M. Grätzel at EPFL, he attended the University of Washington, Seattle, receiving a Ph.D. degree in 1999. He has subsequently worked at the Energy Research Centre Netherlands and is presently a research fellow at the Imperial College, London. His research interests include all aspects of dye-sensitized solar cells, including photophysics, heterogeneous electron transfer, and material science, polymer photovoltaics, and tools for surface characterization of nanostructured interfaces.

**James Durrant** undertook his undergraduate studies in Natural Sciences at the University of Cambridge. For his Ph.D. degree, he studied the primary processes of plant photosynthesis under the supervision of Professors Lord Porter and Jim Barber at Imperial College. In 1999, he joined the Department of Chemistry, Imperial College, London, where he is now Professor of Photochemistry and Deputy Director of the Energy Futures Lab. His research is focused on the photochemical processes that underlie solar energy conversion by nanostructured and molecular materials, harnessing solar energy to produce electricity (photovoltaics) and molecular fuels (e.g., hydrogen).

### FOOTNOTES

*To whom correspondence should be addressed. E-mail: b.oregan@imperial.ac.uk.

### REFERENCES

1 Grätzel, M. Solar energy conversion by dye-sensitized photovoltaic cells. *Inorg. Chem.* **2005**, *44*, 6841–6851.

2 Wang, Q.; Ito, S.; Grätzel, M.; Fabregat-Santiago, F.; Mora-Sero, I.; Bisquert, J.; Bessho, T.; Imai, H. Characteristics of high efficiency dye-sensitized solar cells. *J. Phys. Chem. B* **2006**, *110*, 25210–25221.

3 Ardo, S.; Meyer, G. J. Photodriven heterogeneous charge transfer with transition-metal compounds anchored to $TiO_2$ semiconductor surfaces. *Chem. Soc. Rev.* **2009**, *38*, 115–164.

4 Koops, S. E.; O'Regan, B. C.; Barnes, P. R. F.; Durrant, J. R. Parameters influencing the efficiency of electron injection in dye-sensitized solar cells. *J. Am. Chem. Soc.* **2009**, *131*, 4808–4818.

5 Clifford, J. N.; Palomares, E.; Nazeeruddin, M. K.; Grätzel, M.; Durrant, J. R. Dye dependent regeneration dynamics in dye sensitized nanocrystalline solar cells: Evidence for the formation of a ruthenium bipyridyl cation/iodide intermediate. *J. Phys. Chem. C* **2007**, *111*, 6561–6567.

6 Kroon, J. M.; Bakker, N. J.; Smit, H. J. P.; Liska, P.; Thampi, K. R.; Wang, P.; Zakeeruddin, S. M.; Grätzel, M.; Hinsch, A.; Hore, S.; Wurfel, U.; Sastrawan, R.; Durrant, J. R.; Palomares, E.; Pettersson, H.; Gruszecki, T.; Walter, J.; Skupien, K.; Tulloch, G. E. Nanocrystalline dye-sensitized solar cells having maximum performance. *Prog. Photovoltaics* **2007**, *15*, 1–18.

7 O'Regan, B.; Durrant, J. R.; Sommeling, P.; Bakker, N. J. Influence of the $TiCl_4$ treatment on nanocrystalline $TiO_2$ films in dye-sensitized solar cells. 2. Charge density, band edge shifts, and quantification of recombination losses at short circuit. *J. Phys. Chem. C* **2007**, *111*, 14001–14010.

8 Pelet, S.; Moser, J. E.; Grätzel, M. Cooperative effect of adsorbed cations and iodide on the interception of back electron transfer in the dye sensitization of nanocrystalline $TiO_2$. *J. Phys. Chem. B* **2000**, *104*, 1791–1795.

9 Dor, S.; Grinis, L.; Ruhle, S.; Zaban, A. Electrochemistry in mesoporous electrodes: Influence of nanoporosity on the chemical potential of the electrolyte in dye sensitized solar cells. *J. Phys. Chem. C* **2009**, *113*, 2022–2027.

10 O'Regan, B. C.; López-Duarte, I.; Martinez-Diaz, M. V.; Forneli, A.; Albero, J.; Morandiera, A.; Palomares, E.; Torres, T.; Durrant, J. R. Catalysis of recombination and its limitation on open circuit voltage for dye sensitized photovoltaic cells using phthalocyanine dyes. *J. Am. Chem. Soc.* **2008**, *130*, 2907–2908.

11 Duffy, N. W.; Peter, L. M.; Rajapakse, R. M. G.; Wijayantha, K. G. U. A novel charge extraction method for the study of electron transport and interfacial transfer in dye sensitised solar cells. *Electrochem. Commun.* **2000**, *2*, 658–662.

12 O'Regan, B.; Walley, K.; Juozapavicius, M.; Anderson, A.; Matar, F.; Ghaddar, T. H.; Zakeeruddin, S. M.; Klein, C.; Durrant, J. R. Structure/function relationships in dyes for solar energy conversion. A two atom change in dye structure and the mechanism for its effect on cell voltage. *J. Am. Chem. Soc.* **2008**, *131*, 3541–3548.

13 Ruhle, S.; Greenshtein, M.; Chen, S. G.; Merson, A.; Pizem, H.; Sukenik, C. S.; Cahen, D.; Zaban, A. Molecular adjustment of the electronic properties of nanoporous electrodes in dye-sensitized solar cells. *J. Phys. Chem. B* **2005**, *109*, 18907–18913.

14 O'Regan, B.; Grätzel, M.; Fitzmaurice, D. Optical electrochemistry. 2. Real-time spectroscopy of conduction band electrons in a metal oxide semiconductor electrode. *J. Phys. Chem.* **1991**, *95*, 10525–10528.

15 Rao, C. N. R.; Chat, S. N.; Dwedi, P. C. Spectroscopy of electron donor—acceptor systems. *Appl. Spectrosc. Rev.* **1972**, *5*, 1–170.

16 van de Lagemaat, J.; Frank, A. J. Effect of the surface state distribution on electron transport in dye-sensitized $TiO_2$ solar cells: Nonlinear electron transport kinetics. *J. Phys. Chem. B* **2000**, *104*, 4292–4294.

17 Salvador, P.; Hidalgo, M. G.; Zaban, A.; Bisquert, J. Illumination intensity dependence of the photovoltage in nanostructured $TiO_2$ dye-sensitized solar cells. *J. Phys. Chem. B* **2005**, *109*, 15915–15926.

18 Jennings, J. R.; Ghicov, A.; Peter, L. M.; Schmuki, P.; Walker, A. B. Dye-sensitized solar cells based on oriented $TiO_2$ nanotube arrays: Transport, trapping, and transfer of electrons. *J. Am. Chem. Soc.* **2008**, *130*, 13364–13372.

19 O'Regan, B. C.; Durrant, J. R. Calculation of activation energies for transport and recombination in mesoporous $TiO_2$/dye/electrolyte films taking into account surface charge shifts with temperature. *J. Phys. Chem. B* **2006**, *110*, 8544–8547.

20 O'Regan, B. C.; Lenzmann, F. Charge transport and recombination in a nanoscale interpenetrating network of n-type and p-type semiconductors: Transient photocurrent and photovoltage studies of $TiO_2$/dye/CuSCN photovoltaic cells. *J. Phys. Chem. B* **2004**, *108*, 4342–4350.

21 Peter, L. M. Characterization and modeling of dye-sensitized solar cells. *J. Phys. Chem. C* **2007**, *111*, 6601–6612.

22 Lindquist, S.-E.; Finnstrom, B.; Tegner, L. Photo-electrochemicl properties of polycrystalline $TiO_2$ thin-film electrodes on quartz substrates. *J. Electrochem. Soc.* **1983**, *130*, 351–358.

23 Halme, J.; Boschloo, G.; Hagfeldt, A.; Lund, P. Spectral characteristics of light harvesting, electron injection, and steady-state charge collection in pressed $TiO_2$ dye solar cells. *J. Phys. Chem. C* **2008**, *112*, 5623–5637.

24 Barnes, P. R. F.; Anderson, A. Y.; Koops, S. E.; Durrant, J. R.; O'Regan, B. C. Electron injection efficiency and diffusion length in dye-sensitized solar cells derived from incident photon conversion efficiency measurements. *J. Phys. Chem. C* **2009**, *113*, 1126–1136.

25 Barnes, P. R. F.; Liu, L. X.; Li, X.; Anderson, A. Y.; Kisserwan, H.; Ghaddar, T. H.; Durrant, J. R.; O'Regan, B. C. Re-evaluation of recombination losses in dye-sensitized cells: The failure of dynamic relaxation methods to correctly predict diffusion length in nanoporous photoelectrodes. *Nano Lett.* **2009**, DOI: 10.1021/nl901753k.